ELSEVIER

Thermochimica Acta 385 (2002) 63–71

thermochimica acta

www.elsevier.com/locate/tca

Thermal and structural characterization of cyclomaltononaose (δ-cyclodextrin), cyclomaltodecaose (ε-cyclodextrin) and cyclomaltotetradecaose (ι-cyclodextrin)

Giampiero Bettinetti*, Milena Sorrenti

Dipartimento di Chimica Farmaceutica, Università di Pavia, Viale Taramelli 12, I-27100 Pavia, Italy

Received 23 April 2001; received in revised form 19 July 2001; accepted 19 July 2001

Abstract

Thermal behavior of cyclomaltononaose (δ-cyclodextrin, δ-CD), cyclomaltodecaose (ε-cyclodextrin, ε-CD) and cyclomaltotetradecaose (ι-cyclodextrin, ι-CD) and the solid-state phase transitions associated with the respective dehydration and rehydration processes were investigated. δ-CD, ε-CD and ι-CD in their amorphous and crystalline states were tested by differential scanning calorimetry (DSC), thermogravimetry (TG) and hot stage microscopy (HSM). X-ray powder diffraction (XRD) patterns both experimental and computer generated from single crystal data were used to support thermal data and to follow the solid-state phase transitions associated with thermal dehydration and rehydration of each cyclodextrin (CD). Thermal events associated with dehydration of δ-CD, ε-CD and ι-CD were evaluated and tentatively interpreted on the basis of water arrangements observed in the crystal lattice. Dehydrated δ-CD reverted to the starting $13.75H_2O$ hydrate under high relative humidity (RH) conditions (≈100% RH) at room temperature (RT), while transformed into a $7H_2O$ hydrate at 30–35% RH. Physicochemical characterization based on thermal behavior, which can be related to water arrangements observed in the respective crystals, permits to distinguish between δ-CD, ε-CD and ι-CD, as well as between the amorphous and crystalline states of each CD. The results can be useful for demonstrating the formation of a true inclusion complex of δ-CD, which occurs in two crystalline hydration states, with a guest drug.

Keywords: δ-Cyclodextrin; ε-Cyclodextrin; ι-Cyclodextrin; Thermal analysis; Powder X-ray diffraction; Solid-state phase transition

1. Introduction

Experimental evidence of the occurrence of cyclomaltononaose (δ-cyclodextrin, δ-CD) and higher homologues, commonly referred to as large-ring cyclodextrin (LR-CD), was given in 1957 and 1965 by French and coworkers [1,2], but the complete series of LR-CD from 10 (ε-CD) to 21 (cyclomaltoheinecaose, π-CD) have been isolated, purified and characterized only recently [3–7]. Even larger CD with 26 [8], more than 60 [9], and several hundred [10] of α-1,4-linked δ-glucose units in the macrocycle are described. Crystal structure characterization of δ-CD [11], ε-cyclodextrin (ε-CD) [12], and ι-cyclodextrin (ι-CD) [13] revealed the presence of 13.75, 19 and 9 molecules of crystal water per macrocycle, respec-

Abbreviations: δ-CD, δ-cyclodextrin; ε-CD, ε-cyclodextrin; ι-CD, ι-cyclodextrin; DSC, differential scanning calorimetry; TG, thermogravimetry; HSM, hot stage microscopy; XRD, X-ray powder diffraction; RH, relative humidity; RT, room temperature

* Corresponding author. Tel.: +39-382-507-368; fax: +39-382-507-368.
E-mail address: gpbettinetti@unipv.it (G. Bettinetti).

0040-6031/02/$ – see front matter
PII: S0040-6031(01)00690-6

tively. X-ray analyses of ε-CD and ι-CD crystallized from aqueous solutions, respectively, as 20.3 and 27.3 hydrates have also been reported [14]. In this paper thermal behavior of δ-CD·13.75H_2O, ε-CD·19H_2O and an ι-CD hydrate with ≈18 water molecules per ι-CD molecule was investigated using differential scanning calorimetry (DSC), thermogravimetry (TG) and hot stage microscopy (HSM). Thermal events associated with dehydration were evaluated and tentatively interpreted on the basis of water arrangements observed in the crystal lattice. In addition, thermal data were supported by the X-ray powder diffraction (XRD) patterns (both experimental and computer generated from single crystal data) for characterizing each hydrate in the crystalline and amorphous state. XRD, DSC, and TG were used to follow the solid-state phase transitions associated with thermal dehydration and rehydration of δ-CD, ε-CD, and ι-CD under controlled conditions of relative humidity (RH) at room temperature (RT). Solid-state characterization of δ-CD, ε-CD, and ι-CD could be exploited to characterize the respective inclusion complexes in solid phase with drugs [3,15] and to assess their solid-state interactions with therapeutically important peptides, proteins and oligonucleotides [16,17].

2. Materials and methods

2.1. Materials

Lyophilized δ-CD, ε-CD, and ι-CD samples isolated from CD powder [3–6] were provided by Prof. H. Ueda, Hoshi University, Tokyo.

2.2. Sample preparation

Crystalline δ-CD and ε-CD were prepared from 50% (v/v) aqueous acetonitrile solutions (20 mg_{CD} ml^{-1}) by spontaneous evaporation at RT (∼22 °C). Crystalline ι-CD was obtained by evaporation of a 7:3 (v/v) water/1-propanol solution (2 $mg_{\iota\text{-CD}}$ ml^{-1}) under the same experimental conditions. Rehydration of samples scanned to 180 °C by DSC (see later) was carried out in a desiccator kept at a RH of 30–35% or ≈100% by equilibrating at RT over a saturated solution of $CaCl_2·6H_2O$ or pure water, respectively.

2.3. Thermal analysis

Temperature and enthalpy values were measured with a METTLER STAR[e] system equipped with a DSC821[e] Module on 3–4 mg (Mettler M3 Microbalance) samples in uncovered Al pans under static air. An uncovered empty pan was used as reference. The heating rate was 10 K min^{-1} over the 30–330 °C temperature range. The instrument was calibrated with a standard sample of indium (purity: 99.99%, melting point: 156.9 °C, $\Delta H = 28.05$ J g^{-1}). Some samples were scanned to 180 °C, rehydrated in their pans at RT by exposure to 30–35% or ≈100% RH to a constant weight, and rescanned over the 30–180 °C temperature range. The experiments were carried out at least in duplicate.

Mass losses were recorded with a Mettler TA 4000 apparatus equipped with a TG 50 cell at the heating rate of 10 K min^{-1} on 6–8 mg samples in open alumina crucibles over the 30–330 °C temperature range under static air. Temperature was calibrated by the Curie point temperature of standard metals (alumel (149.3 °C), nickel (357 °C), trafoperm (745.6 °C)). The experiments were carried out at least in duplicate.

Microscopic observation of the sample morphology and thermal events on heating were carried out under a Reichert polarized light microscope equipped with a Mettler FP82HT/FP80 system at a heating rate of 10 K min^{-1}. Images were transferred via a Panasonic WV-CP100E CCTV camera to a Panasonic WC-CH110A video monitor and to a PowerPC Macintosh computer for elaboration (ADOBE PHOTOSHOP 5.0).

2.4. X-ray diffraction measurements

The unit cell data for δ-CD [10], ε-CD [11], and ι-CD [12] were used as input to the program LAZY PULVERIX [18] to generate the idealized powder XRD patterns for these species. Experimental powder XRD patterns were taken at ambient temperature and atmosphere with a Philips PW 1800/10 apparatus equipped with specific PC-APD software with powdered samples mixed with ≈100 mg of NaF placed in Al holders. Wavelengths: Cu $K\alpha_1 = 1.54060$ Å, and Cu $K\alpha_2 = 1.54439$ Å. Scan range: $2\theta = 2$–$50°$. Scan speed: $2\theta = 0.02° \, s^{-1}$. Monochromator: graphite crystal.

3. Results and discussion

3.1. Cyclomaltononaose (δ-cyclodextrin, δ-CD)

Thermal and XRD results for δ-CD are presented in Figs. 1 and 2. Lyophilized, X-ray amorphous (Fig. 2a) δ-CD exhibits a broad DSC dehydration endotherm (peak A), which is attributable to sorbed water release, and an endothermal deflection of the baseline at 270 °C (peak B) due to sample decomposition (Fig. 1, DSC curve a). A mass loss over the temperature range of the DSC endotherm of $11.6 \pm 0.2\%$ (w/w), which corresponds to liberation of ≈11 water molecules per δ-CD molecule, was calculated by TG (Fig. 1, TG curve a). Crystals by slow evaporation of a 50% (v/v) aqueous acetonitrile solution show an XRD pattern (Fig. 2b) which was in good agreement with the theoretical pattern (Fig. 2b*) calculated from single crystal data for δ-CD·13.75H_2O [10]. Five water molecules in the asymmetric unit are in fully occupied state and lay around the wide space at the O6 side, whereas the rest 8.75 water molecules are in disordered state and stay at the narrow space of O6 side, forming a water cluster by hydrogen bonds [10]. δ-CD·13.75H_2O shows a broad DSC endotherm from 30 to 130 °C attributable to water of hydration release, with a peak A emerging from 49 to 87 °C ($T_{peak} = 64 \pm 4$ °C, enthalpy change $\Delta H = 114 \pm 12$ J g^{-1}) and a subsequent exothermal effect with peak maximum temperature at 128 °C (peak B) possibly due to rearrangement of the δ-CD dehydrated structure, which represents the stable form

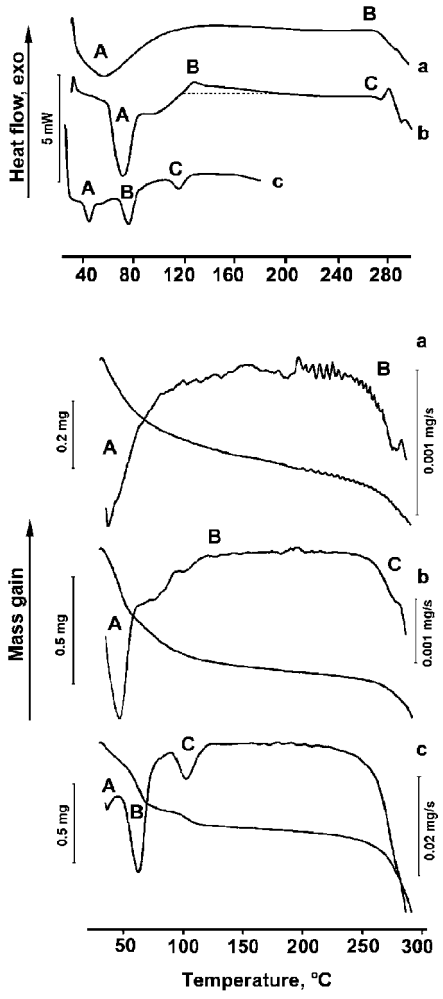

Fig. 1. DSC (upper curves), TG and dTG (lower curves) of δ-CD. Key: (a) amorphous δ-CD; (b) δ-CD·13.75H_2O; (c) δ-CD·7H_2O.

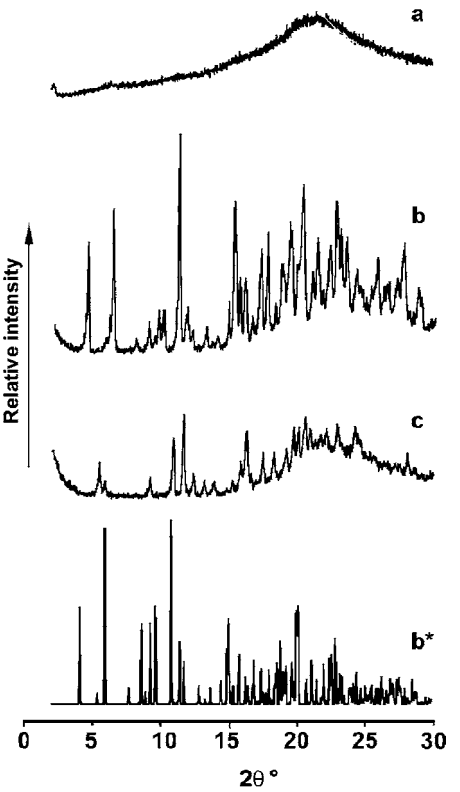

Fig. 2. XRD patterns of δ-CD. Key: (a) amorphous δ-CD; (b) δ-CD·13.75H_2O; (c) δ-CD·7H_2O; (b*) computer generated from single crystal data of δ-CD·13.75H_2O.

over the 128–270 °C temperature range (Fig. 1, DSC curve b). The next exotherm with peak maximum temperature at 282 °C (peak C) may be ascribed to decomposition of δ-CD anhydrate melt formed at 270.5 °C, in correspondence with the endothermal deflection of the baseline. The DSC pattern was reflected by the TG and first-derivative TG (dTG) curves (Fig. 1b), indicating that each mass loss by dehydration was associated with a definite energy uptake. The mass loss of $8 \pm 1\%$ (w/w) from 30 to 62 °C (the lower DSC integration limit of the first thermal effect A) corresponds to escape of ≈9 mol of water, i.e. those present in disordered state in the crystal lattice. The subsequent mass loss from 62 to 120 °C of $6 \pm 1\%$ (w/w) can be ascribed to elimination of the 5 mol of water in fully occupied state (i.e. more tightly bound) in the crystal lattice. The total TG mass loss of $14.6 \pm 0.4\%$ (w/w) over the 30–250 °C range was in good agreement with the theoretical value for $C_{54}H_{90}O_{45}{\cdot}13.75H_2O$, F.W. 1707 (14.5% as water mass fraction).

Fig. 3 is a composite HSM photograph of a δ-CD·$13.75H_2O$ crystal immersed in high-boiling silicone oil at several temperatures from 25 to 285 °C. The crystal, which is colorless at 25 °C and pale blue at 75 °C, starts to crack at 110 °C with liberation of bubbles from the center at 160 °C corresponding to the escape of water vapor. The higher desolvation temperature under HSM than by TG or DSC is probably due to suppression of dehydration by the surrounding oily medium. Upon further heating, the crystal expands with the appearance of bubbles in the center

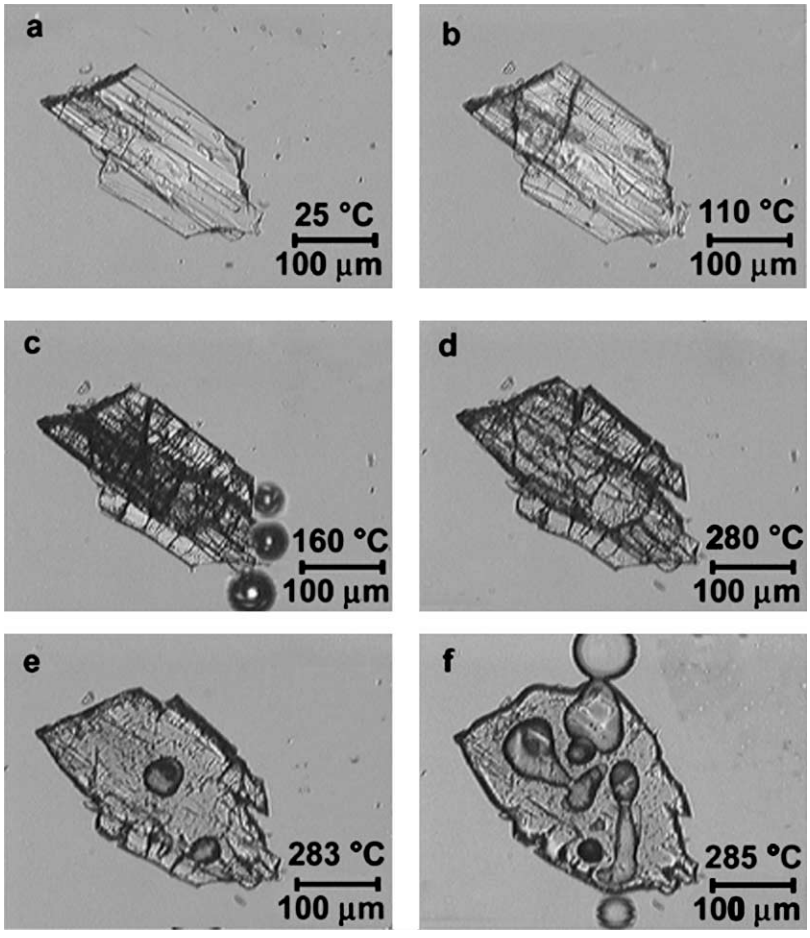

Fig. 3. Microphotographs of δ-CD·$13.75H_2O$ at various temperatures taken with hot stage microscopy.

due to simultaneous melting and decomposition of the dehydrated δ-CD at 285 °C.

XRD patterns of the rehydration products of dehydrated δ-CD·13.75H_2O (see Section 2.2) showed that under high RH conditions (≈100% RH, RT) the starting hydrate was obtained (pattern not shown), whereas under lower RH conditions (30–35% RH, RT) a differing hydrated phase was formed (Fig. 2c). As can be seen in Fig. 1, this product was characterized by a DSC curve c with a triplet of resolved dehydration endotherms A (from 33 to 61 °C; $T_{peak,A} = 45.3 \pm 0.7$ °C, enthalpy change $\Delta H_A = 29.8 \pm 0.7$ J g^{-1}), B (from 63 to 87 °C; $T_{peak,B} = 76.3 \pm 0.3$ °C, enthalpy change $\Delta H_B = 57 \pm 4$ J g^{-1}), and C (from 99 to 103 °C; $T_{peak,C} = 115.4 \pm 0.7$ °C, enthalpy change $\Delta H_C = 25 \pm 5$ J g^{-1}). The DSC peaks were reflected by TG inflection points and dTG peaks with associated mass losses of 1.7 ± 0.15, 4.7 ± 0.3, and 1.3 ± 0.2% (w/w) over the temperature range shown, respectively, for peaks A, B, and C (Fig. 1, TG curve c). The TG mass loss over the 30–250 °C range of 7.8 ± 0.3% corresponded to the presence of about seven water molecules per δ-CD molecule, i.e. to a heptahydrate stoichiometry ($C_{54}H_{90}O_{45}$·7H_2O, F.W. 1585.5: theoretical value 7.95% as water mass fraction). The stepwise water loss of 1.5, 4.5, and 1 mol of water over the 33–103 °C range suggests the presence of three different water environments in the heptahydrated crystal structure.

3.2. Cyclomaltodecaose (ε-cyclodextrin, ε-CD)

Thermal and XRD results for ε-CD show that lyophilized, X-ray amorphous (Fig. 4, pattern a) ε-CD exhibits a broad DSC dehydration endotherm attributable to sorbed water release (peak A), and a following endo–exothermal effect due sample decomposition at 280 °C (peak B) (Fig. 4, DSC curve a). The TG mass loss of 10 ± 1% (w/w) associated with peak A (Fig. 4, TG curve a) corresponds to ≈11 mol of water, practically the same amount released by amorphous δ-CD (see Fig. 1, TG curve a). Crystals from a 50% (v/v) aqueous acetonitrile solution show a XRD pattern (Fig. 4b) in reasonably good agreement with the theoretical pattern (Fig. 4b*) from ε-CD·19H_2O single crystal data [11], except differences in the relative intensity of some peaks attributable to preferred orientation effects [19]. Of the 10 water molecules in the asymmetric unit of ε-CD·19H_2O, which contains half a molecule the second half being related by crystallographic symmetry, three are located inside the ε-CD cavity and seven in the interstices between the macrocycles [11]. As shown by the DSC curve

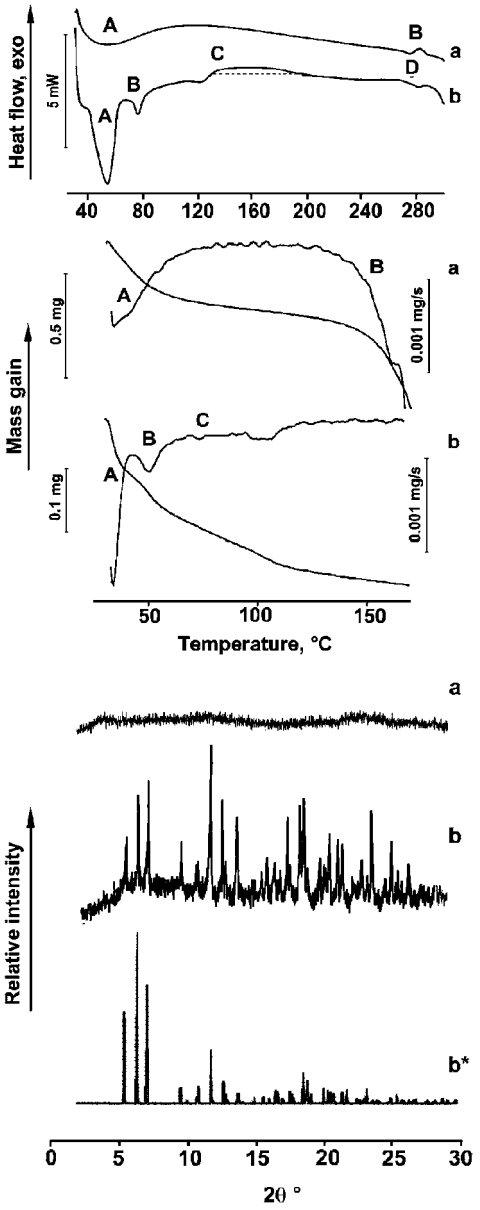

Fig. 4. DSC (upper curves), TG and dTG (middle curves) and XRD patterns (lower curves) of ε-CD. Key: (a) amorphous ε-CD; (b) ε-CD·19H_2O; (b*) computer generated from single crystal data of ε-CD·19H_2O.

(Fig. 4b) crystalline ε-CD shows two separate DSC endothermal effects A (from 38 to 65 °C; $T_{peak,A} = 60 \pm 5$ °C, enthalpy change $\Delta H_A = 231 \pm 12$ J g^{-1}) and B (from 65 to 86 °C; $T_{peak,B} = 76 \pm 1$ °C, enthalpy change $\Delta H_B = 27 \pm 3$ J g^{-1}), and just after the total loss of water, an exothermal effect C at 135 °C. On the analogy of δ-CD·13.75H_2O this effect, that extends to 235 °C and is followed by simultaneous melting and decomposition at 268 °C, D, can be attributed to rearrangement of the ε-CD dehydrated structure. The TG and dTG curves (Fig. 4b) recorded over the 30–180 °C range reflected the multi-step dehydration observed in DSC runs. The mass loss of $4.4 \pm 0.3\%$ (w/w) from 30 to 38 °C (the lower DSC integration limit of peak A) corresponded to escape of 5 mol of water, as many as those associated to the mass loss of $4.8 \pm 0.4\%$ (w/w) from 38 to 65 °C, i.e. over the DSC integration limits of peak A. The subsequent mass losses of $1.8 \pm 0.2\%$ w/w from 65 to 86 °C (the DSC integration limits of peak B), $2.8 \pm 0.3\%$ (w/w) from 86 to 120 °C, and $1.8 \pm 0.2\%$ from 120 to 150 °C corresponded to elimination of 2, 3, and 2 mol of water, respectively. The rest of water molecules, most likely the two which have the largest temperature factors in the crystal lattice, are lost when ε-CD·19H_2O is exposed to ambient atmosphere. The TG mass loss over the 30–180 °C range of $17.7 \pm 0.5\%$ (w/w) was in good agreement with the theoretical value for $C_{60}H_{100}O_{50}$·19H_2O, F.W. 1962.3 (17.4% as water mass fraction).

Fig. 5 is a composite HSM photograph of a ε-CD·19H_2O crystal immersed in high-boiling silicone oil at several temperatures from 25 to 270 °C. The crystal, which in polarized light at 25 °C appears pink in some parts and blue in others, maintains its shape and color up to 190 °C, when it becomes totally blue. On further heating the crystal becomes colorless at 240 °C and maintains its shape until just before 260 °C, when its edges become round and bubbles start evolving from the lower side. The liberation of bubbles continued at progressively higher rate until simultaneous melting and decomposition at 270 °C. As for δ-CD·13.75H_2O, the higher temperature of escape of water vapor from the crystal under HSM than by TG or DSC is probably due to suppression of dehydration by the surrounding oily medium.

Rehydration of dehydrated ε-CD·19H_2O (see Section 2.2) under high RH (≈100% RH, RT) or

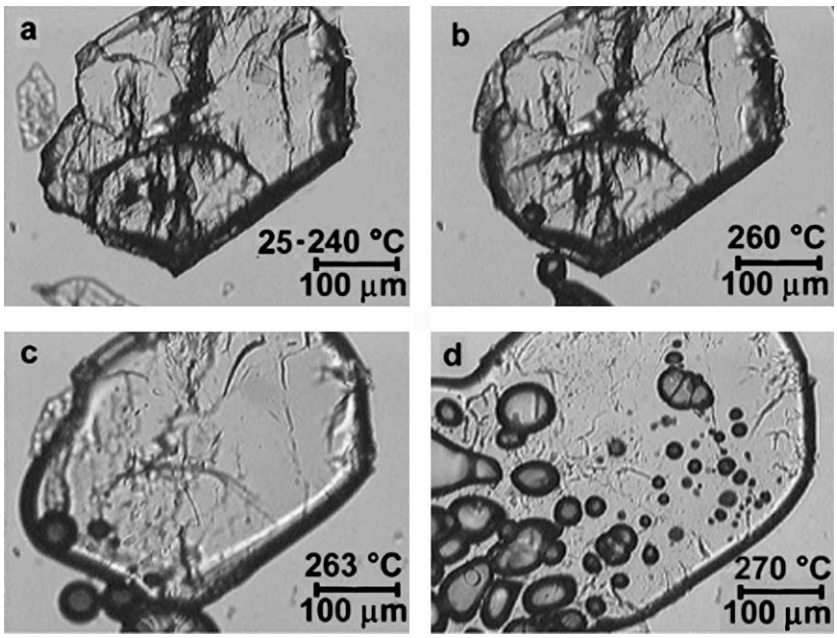

Fig. 5. Microphotographs of ε-CD·19H_2O at various temperatures taken with hot stage microscopy.

ambient (30–35% RH, RT) conditions gave products which showed similar DSC profiles (not shown) as the starting hydrate.

3.3. Cyclomaltotetradecaose (ι-cyclodextrin, ι-CD)

Thermal and XRD results for ι-CD show that lyophilized, X-ray amorphous (Fig. 6, pattern a) ι-CD is characterized by a broad DSC dehydration endotherm (peak A) as the counterparts ε-CD and δ-CD (see Figs. 1 and 4, DSC curves a), but after the sorbed water release, a characteristic glass transition ($T_{\text{mid-point}} = 174.2 \pm 0.5\,^{\circ}\text{C}$) (peak B) between 171 and 177 °C and a following exothermal decomposition with a peak maximum temperature at 280 °C (peak C) can be seen (Fig. 6, DSC curve a). Crystals from 7:3 (v/v) water/1-propanol solution show an XRD pattern (Fig. 6b) which was in reasonably good agreement with the theoretical pattern (Fig. 6b*) from ι-CD·9H_2O single crystal data [12], except differences in the relative intensity of some peaks attributable to preferred orientation effects [19]. In the asymmetric unit of ι-CD·9H_2O, which contains half a molecule the second half being related by crystallographic symmetry, only one of the five molecules of water involved in the hydrogen bond network in the crystal, that located inside the ι-CD ring, is in a monomeric state, i.e. not linked to any other water molecules [12]. Crystalline ι-CD (Fig. 6, DSC curve b) shows a broad DSC endothermal effect (peak A) from 37 to 64 °C ($T_{\text{peak}} = 48.5 \pm 0.3\,^{\circ}\text{C}$, enthalpy change $\Delta H = 80 \pm 20\ \text{J g}^{-1}$) with a shoulder (peak B) at 66 °C, which is followed by a broad exothermal effect (peak C) with peak maximum temperature at 102 °C and endothermal deflection of the baseline at 282 °C (peak D) due to melting with decomposition of ι-CD anhydrate. So, a rearrangement of the dehydrated structure analogous to that observed for δ-CD and ε-CD was displayed also by ι-CD.

The TG mass loss over the 30–180 °C range of $12.8 \pm 0.5\%$ (w/w) (Fig. 6, TG curve b) was in agreement with the theoretical value for $C_{84}H_{140}O_{70}\cdot 18H_2O$, F.W. 2594.1 (12.50% as water mass fraction). Actually, ι-CD is reported to be able to link up to 27.3 water molecules with no substantial alteration of its monoclinic unit cell [14], in agreement with our experimental results which show its ability to link a very variable number of water molecules depending on the crystallization and/or atmospheric humidity conditions. Following the DSC and TG profiles (Fig. 6, curve b), the mass loss of $2.9 \pm 0.2\%$ (w/w)

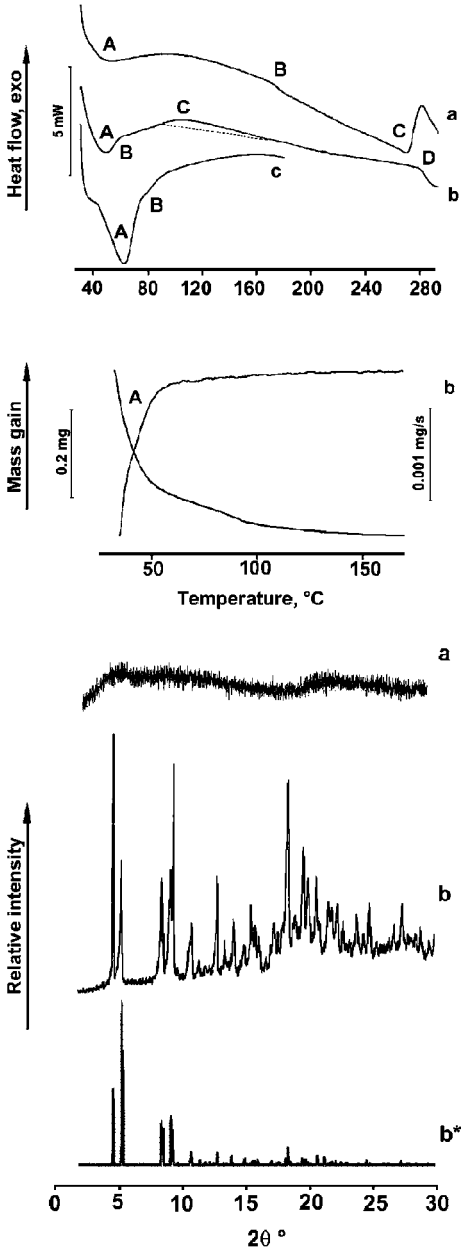

Fig. 6. DSC (upper curves), TG and dTG (middle curves) and XRD patterns (lower curves) of ι-CD. Key: (a) amorphous ι-CD; (b) crystalline ι-CD hydrate (18H_2O per ι-CD molecule by TG); (b*) computer generated from single crystal data of ι-CD·9H_2O; (c) rehydrate ι-CD by exposure to 30–35% RH conditions at RT.

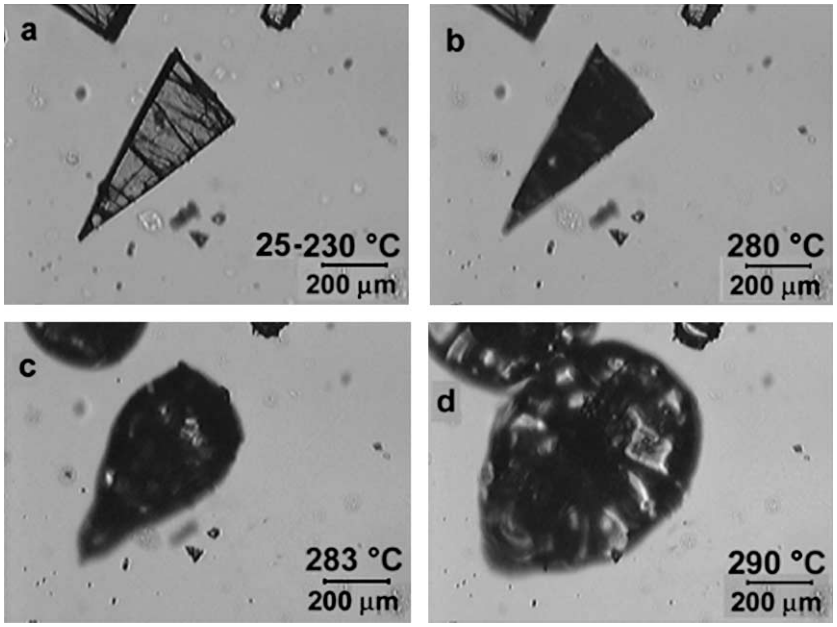

Fig. 7. Microphotographs of crystalline ι-CD hydrate ($18H_2O$ per ι-CD molecule by TG) at various temperatures taken with hot stage microscopy.

from 30 to 37 °C (the lower DSC integration limit of peak A) corresponds to escape of ≈4 mol of water, that from 37 to 66 °C (the DSC integration limits of peak A) of 5.8 ± 0.3% (w/w) to elimination of ≈8 mol of water, and those from 66 to 102 °C (2.1 ± 0.3% w/w) and from 102 to 170 °C (1.8 ± 0.2% w/w) to a two-step liberation of 6 mol of water.

Fig. 7 is a composite HSM photograph of a ι-CD·$18H_2O$ hydrate crystal (by TG) immersed in high-boiling silicone oil at several temperatures from 25 to 290 °C. The isosceles-triangle shaped crystal changes color at 230 °C, probably in correspondence to a phase transformation to the anhydrate, though bubbles did not appear due to a possible suppression a possible of dehydration by the surrounding oily medium as already postulated for ε-CD·$19H_2O$ and δ-CD·$13.75H_2O$ crystals. The crystal habit does not change until 280 °C, but upon further heating gradually expands due to simultaneous melting and decomposition.

Rehydration of dehydrated crystals of ι-CD (see Section 2.2) under 30–35% RH conditions at RT gave a product with a similar DSC profile (not shown) as the starting hydrate. The DSC dehydration endotherm with peak maximum temperature at 62 °C (peak A) and a shoulder at 80 °C (peak B) was however, sharper and more symmetric than that recorded for the original sample (Fig. 6, DSC curve c). This allowed us to more accurately evaluate the associated dehydration enthalpy ($\Delta H = 166 \pm 8$ J g^{-1}) in the 40–77 °C range.

4. Conclusions

In contrast to ε-CD which is a very weak complex former with a number of potential guest [15], δ-CD shows specific complexing and solubilizing capacities toward various drugs [3,20], slightly water-soluble substances [21], and macrocyclic compounds [22]. δ-CD is not commercially available at present, though both purity and yields were improved [23], and alternative sources where δ-CD was formed in the range 5–11.5% of the total amount of all CD produced were found [24,25]. Therefore, in light of the possible availability of δ-CD on a larger scale in the near future, its pharmaceutical applications as complexing agent for drug molecules of suitable geometries can be foreseen. In this perspective, characterization of the solid-state properties of δ-CD, which can be isolated

in two crystalline hydrated states, can be useful in the study of solid-state interactions with drugs, in particular for demonstrating the formation of a true drug/δ-CD inclusion complex.

Acknowledgements

The authors wish to thank Prof. R. Mino Caira of the University of Cape Town (South Africa) for calculation of the theoretical XRD patterns and Prof. Haruhisa Ueda of the Hoshi University (Tokyo) for his kind cooperation. Financial support from FAR (Fondo di Ateneo per la Ricerca Scientifica) is gratefully acknowledged.

References

[1] D. French, in: M.L. Wolfrom (Ed.), Advances in Carbohydrate Chemistry, Vol. 12, New York, 1957, p. 205.
[2] D. French, A.O. Pulley, J.A. Effenberger, M.A. Rougvie, M. Abdullah, Archiv. Biochem. Biophys. 111 (1965) 153.
[3] I. Miyazawa, H. Ueda, H. Nagase, T. Endo, S. Kobayashi, T. Nagai, Eur. J. Pharm. Sci. 3 (1995) 153.
[4] T. Endo, H. Ueda, S. Kobayashi, T. Nagai, Carbohydrate Res. 269 (1995) 369.
[5] T. Endo, H. Nagase, H. Ueda, S. Kobayashi, T. Nagai, Chem. Pharm. Bull. 45 (1997) 532.
[6] T. Endo, H. Nagase, H. Ueda, A. Shigihara, S. Kobayashi, T. Nagai, Chem. Pharm. Bull. 45 (1997) 1856.
[7] T. Endo, H. Nagase, H. Ueda, H. Shigihara, S. Kobayashi, T. Nagai, Chem. Pharm. Bull. 46 (1998) 1840.
[8] K. Gessler, I. Uson, T. Takaha, N. Krauss, S.M. Smith, S. Okada, G.M. Sheldrick, W. Saenger, Proc. Natl. Acad. Sci. U.S.A. 96 (1999) 4246.
[9] Y. Terada, M. Yanase, H. Takata, T. Takaha, S. Okada, J. Biol. Chem. 272 (1997) 15729.
[10] T. Takaha, M. Yanase, H. Takata, S. Okada, S.M. Smith, J. Biol. Chem. 271 (1996) 2902.
[11] T. Fujiwara, N. Tanaka, S. Kobayashi, Chem. Lett. (1990) 739.
[12] H. Ueda, T. Endo, H. Nagase, S. Kobayashi, T. Nagai, J. Incl. Phenom. 25 (1996) 17.
[13] K. Harata, T. Endo, H. Ueda, T. Nagai, Supramol. Chem. 9 (1998) 143.
[14] J. Jacob, K. Gessler, D. Hoffmann, H. Sanbe, K. Koizumi, S.M. Smith, T. Takaha, Angew. Chem. Int. Ed. 37 (1998) 606.
[15] K.L. Larsen, H. Ueda, W. Zimmermann, Carbohydrate Res. 309 (1998) 153.
[16] B. Haeberlin, T. Gengenbacher, A. Meinzer, G. Fricker, Int. J. Pharm. 137 (1996) 103.
[17] T. Irie, K. Uekama, Adv. Drug Delivery Rev. 36 (1999) 101.
[18] K. Yvon, W. Jeitschko, E.J. Parthe, J. Appl. Crystallogr. 10 (1977) 73.
[19] R. Suryanarayanan, X-ray powder diffractometry, in: H.G. Brittain (Ed.), Physical Characterization of Pharmaceutical Solids, Marcel Dekker, New York, 1995, pp. 190, 194, 214.
[20] H. Ueda, A. Wakamiya, T. Endo, H. Nagase, K. Tomono, T. Nagai, Drug Dev. Ind. Pharm. 25 (1999) 951.
[21] T. Furuishi, T. Endo, H. Nagase, H. Ueda, T. Nagai, Chem. Pharm. Bull. 46 (1998) 1658.
[22] H. Akasaka, T. Endo, H. Nagase, H. Ueda, S. Kobayashi, Chem. Pharm. Bull. 48 (2000) 1986.
[23] A. Wakamiya, T. Endo, H. Nagase, H. Ueda, S. Kobayashi, T. Nagai, Yakuzaigaku 57 (1997) 220.
[24] K.L. Larsen, L. Duedahal-Olsen, H.J.S. Christensen, F. Mathiesen, L.H. Pedersen, W. Zimmermann, Carbohydrate Res. 310 (1998) 211.
[25] K.L. Larsen, H.J.S. Christensen, F. Mathiesen, L.H. Pedersen, W. Zimmermann, Appl. Microbiol. Biotechnol. 50 (1998) 314.